The origin of moisture feeding up Atmospheric Rivers over the Arctic

Marta Vázquez [1]*, Karina Pereira [1], Raquel Nieto [1,2] and Luis Gimeno [1]

Published: 05/11/2017
Academic Editor: Ricardo Trigo

[1] Environmental Physics Laboratory (EPhysLab), Facultade de Ciencias, Universidade de Vigo, Ourense 32004, Spain; karinapereiramartinez@hotmail.com (K.P.); rnieto@uvigo.es (R.N.); l.gimeno@uvigo.es (L.G.)

[2] Departmento of Atmospheric Sciences, Institute of Astronomy, Geophysics Atmospheric Sciences, Universitu of Sao Paulo 05508-090, Brazil

* Correspondence: martavazquez@uvigo.es

Abstract: The Arctic system is one of the most vulnerable regions under climate change conditions and it has suffered important changes on last decades. Several recent studies have suggested the influence of moisture transport in the observed sea ice loss in this region. Atmospheric rives (ARs) represent one of the main mechanism of global moisture transport, being especially relevant in the connection between lower and higher latitudes. The objective of this is work is to identify the main areas where the moisture is anomalously uptake for the ARs that reach the Arctic polar region. For this purpose, the lagrangian model FLEXPART was used to analyse moisture sources for those regions of maximum occurrence of ARs to the Arctic for the period 1997-2014 in order to analyse the anomalous origin of moisture transported by these meteorological structures. The region of maximum occurrence of ARs was defined taking into account the number of the systems that reach 60ºN during August and September when sea ice is minimum over the Arctic Ocean. For these regions and considering those days of ARs occurrence, the anomalous moisture sources were defined in relation to the mean situation for the complete period. From the results, main moisture sources for ARs events extends over the North Atlantic and North Pacific oceans, moreover, local input of moisture over the region of maximum ARs occurrence seems to be especially relevant. It is interesting to highlight the moisture uptake from Eastern Asia during August. In general, it could be conclude that for ARs events the moisture uptake around and over the maximum occurrence area highly increase becoming relevant sources of moisture feeding up the event.

1. Introduction

The Arctic is suffering for important changes in recent decades associated with the climate change. One of the most relevant change observed over this region is the extreme reduction in sea ice, which has shown a downward trend in its extent in the last few decades for all seasons [1-4] and being the decrease more pronounced on late summer [5-6], when sea ice reaches its minimum annual value. Several recent studies have investigated the causes of this decrease, being changes in moisture transport from lower latitudes one of the possible factors suggested to affect the region [7-9].

Multiple mechanisms are responsible for the global moisture transport, being the Atmospheric Rivers (ARs) one of the most important. ARs are long and narrow corridors, which transport water vapour meridionally from lower to higher latitudes. Despite covering only approximately 10 % of the Earth's circumference, these atmospheric structures account for over 90% of the total poleward water vapour transport at midlatitudes [10] and are associated with extreme events of precipitation [11-14]. Gimeno et al. [15] have realized a minireview of the general characteristics of ARs.

According to Sorterberg and Walsh [16], interannual variability on moisture transport toward the Arctic is mainly related to the variability on cyclone activity over the Greenland Sea and Eastern Siberian Sea, and of course, ARs are absolutely related with the cyclone activity in these latitudes. Despite its formation may be independent of the genesis and development of cyclones, cyclone activity may have an influence on ARs development [10].

Despite the importance of ARs in moisture transport, and their influence in the Arctic warming [e.g., 17], their influence on the Arctic region have not already been deeply investigated in these terms pointed here. The aim of this work is to establish the first step for a more complete analysis about those areas that support anomalous moisture to the Arctic ARs. For this purpose, and employing the lagrangian model FLEXPART, the origin of the anomalous moisture vapour feeding up the ARs at 60°N is analysed for August and September during the period 1997-2014.

2. Experiments

3.1. Location of the maximum occurrence regions of ARs.

In order to investigate the ARs that affect the Arctic region, the ARs database developed by Guan and Waliser [18] was used. This database provide the ARs position on a global scale with 1°x1° horizontal resolution along the year with a time step of 6 hours (00, 06, 12, 18 UTC). AR detection is based on the computing of the vertically integrated horizontal water vapour transport (IVT) between 1000 and 300 hPa, taking into account the specific humidity and wind field retrieved from the ECMWF Interim reanalysis (ERA-Interim) [19]. At each grid cell, the 85th percentile is applied as a threshold with a fixed lower limit of 100 kgm^{-1}s^{-1} (for polar regions). Once the threshold has been applied, the coherence on the IVT direction is analysed by discarding those regions with more than half of the grid cells showing deviations of more than 45° from the mean IVT and those that do not have an appreciated poleward component. From this procedure a set of ARs is detected. Further details can be found at Guan and Waliser [18].

From the previous database, the regions of maximum occurrence of ARs are identified for August and September for the period 1997-2014. In order to analyse the ARs affecting the Arctic we considered only those systems that reach a 10° latitudinal band centered on 60°N around all the Arctic. Then, over this band, we detect the areas of maximum occurrence of ARs as those with more ARs than the 75th percentile of it monthly frequency.

3.2. Moisture sources

The lagrangian model FLEXPART v9.0 [20-21] is applied to analysed the moisture sources for the areas of maximum AR occurrence previously defined. FLEXPART uses ERA-Interim reanalysis data on 1° horizontal resolution to track the atmospheric moisture. The atmosphere is divided into air parcels (or particles) which are dispersed following the 3-D wind field. For every air parcel the specific humidity (q) and the position is stored every 6 hours and moisture changes can be expressed as

$$e - p = m\frac{dq}{dt}$$

representing e and p moisture increases and decreases, m the mass of the particle and t the time. If the (e-p) for all the particles at every grid position is considered it can be obtained the total surface freshwater flux (E-P), being (E) and (P) the rates of evaporation and precipitation per unit area respectively.

FLEXPART model can be applied to follow particles backward and forward in time. Backward modelling allows the location of moisture sources for specific regions. In this case, to localize the sources of moisture for the ARs maximum occurrence areas, the particles were followed backward in time for 10 days (the average residence time of water vapour in the atmosphere [22].

In order to analyse the anomalous moisture uptake associated with ARs reaching the Arctic, the method employed by Ramos et al. [23] was applied. Following this methodology backward trajectories were followed for 10 days at 6h intervals (40 time steps) for every of the ARs cases. With the purpose of compute the moisture uptake, only positive values of (E-P) were retained at each and every time step. The area of anomalous moisture uptake was obtained by computing the anomaly between (a) the total (E-P) > 0, considering every case of ARs occurrence at 6h intervals (taking into account the 10 days backward trajectories) and (b) the 'climatology' for the corresponding ARs cases. On this work, an AR case will be defined as every one of the times on which an AR occurs at 6 hours interval. For example, if an AR takes place from 00:00 UTC to 18:00 UTC on 15 September 1999, 4 AR cases will be considered (00, 06, 12 and 18 UTC). The climatology is calculated considering only the dates of ARs occurrence but for all the 18-year period in consideration in this study, 1997-2014. For instance, if an AR case was detected on 15 September 1999 at 12:00 UTC, the climatology will consider the 15 September at 12:00 for every year of the period 1997-2014. As previously explained, only positive values of E-P were considering at every of the 40-time steps (10 days backward every 6 hours). This climatological value will be denoted hereinafter as $(E-P)_{CLI} > 0$. The anomaly is calculated by the difference between (a) and (b) and it is denoted as $(E-P)_{AN} > 0$.

3. Results and discussion

In order to define the areas of maximum ARs occurrence, figure 1 shows the number of ARs for each longitude from 55°N to 65°N and their geographical distribution for August and September. On this figure, blue line represents the longitudinal variability on the number of ARs and the horizontal red line represents the value of its 75th percentile. Embedded at the bottom on this figure, ARs frequency appears represented for every grid point over the longitudinal band previously defined. On this plot, reddish colours represent higher ARs occurrence and bluish colours lower ARs frequency.
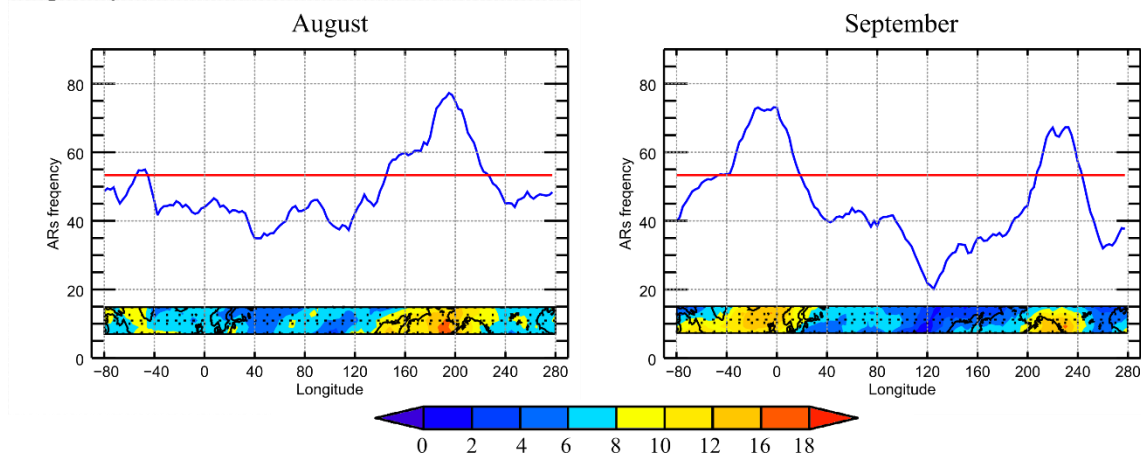

Figure 1. ARs occurrence over the area between 55 and 65°N for August and September over the period 1997-2014. The blue line represents the number of ARs for every longitude and the box embedded in the plot show the spatial distribution of ARs. Reddish colours represent the areas with higher AR occurrence and bluish colours those with the lower occurrence.

Taking into account only those regions where the ARs number exceed the 75th percentile, the areas of maximum occurrence can be defined. In August the maximum ARs frequency occurs over the Pacific Ocean, between 142.5 – 225.5°E, affecting the Bering Sea, the Sea of Okhotsk and western Alaska. For this month, a very small isolated area of high values of ARs appears over the Davis Strait, however considering the small area it represents and the low values compared with the Pacific region, this area was not taking into consideration. For September two important areas of ARs occurrence can be found, one over the Atlantic Ocean, and another over the Pacific. Over the Pacific, higher values occur between 207.5 and 242.5°E, over the Gulf of Alaska, and for the Atlantic Ocean between -37.5°W and 15°E.

Once the areas of maximum occurrence were defined for each month, it is possible to analyse their sources of moisture. For this purpose, figure 2 shows the climatological sources (those regions with $(E-P)_{CLI} > 0$ values) for both months in the period 1997-2014. On August, most of the moisture reaching the pacific area of maximum ARs occurrence is mainly taken from the continental areas inside and around it. Highest values on $(E-P)_{CLI}$ occur over Alaska, Russian Far East, and eastern China. Some moisture is also provided by the Pacific Ocean, in a band between 25-40° N approximately. On September most of the moisture contribution comes from oceanic areas. The Pacific maximum occurrence area is supplied by moisture from the northern Pacific. In the case of the Atlantic area, main moisture source is located along the Atlantic Ocean on the path of northern hemisphere cyclones. Moreover, this latest area receives moisture from continental areas over North America and Europe, despite their contribution is lower than the oceanic one.
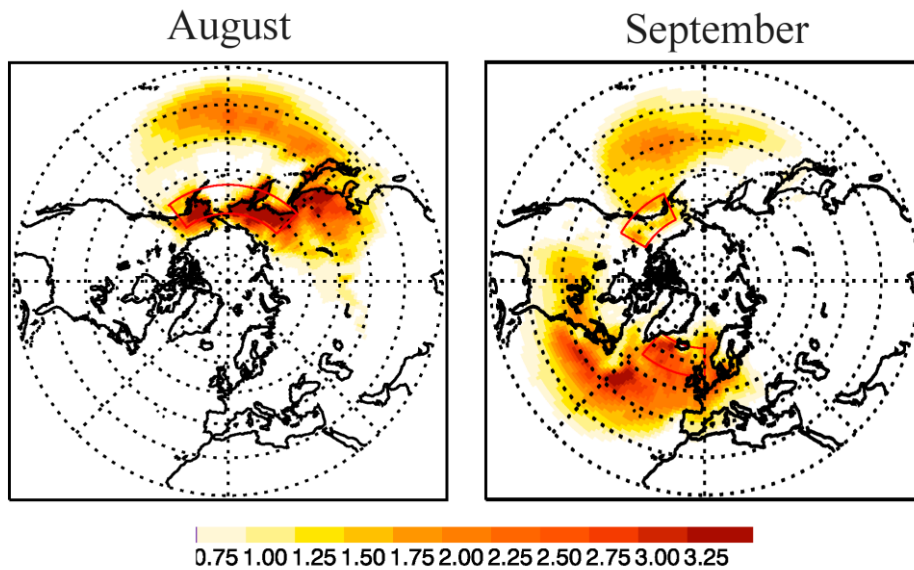

Figure 2. Moisture sources ($(E-P)_{CLI}>0$ regions) calculated for August and September over the period 1997-2014 for regions of maximum ARs occurrence represented by the red boxes. Scale in mm/day.

Finally, figure 3 shows the anomaly on (E-P) for ARs cases ($(E-P)_{AN} > 0$). As explained before only the specific times of AR occurrence are taking into consideration for the calculation. The number of AR cases considered for every region and month are shown on Table 1.

Table 1. Number ARs cases detected by month over the period 1997-2014 for each region of maximum occurrence.

	August	September
Pacific Ocean	1677	1173
Atlantic Ocean		616

In August, it can be observed as almost the total of the climatological sources increased its moisture uptake during ARs events. Despite positive anomalies can be found over the Pacific Ocean, the higher increases appear over continental areas, coinciding with those areas showing higher (E-P)$_{CLI}$ values on the climatological results. In September, general increases in the moisture sources can be observed, as in August, for both Pacific and Atlantic areas. This increase, for the Atlantic area of maximum occurrence, is higher over the region itself and gradually decreases with the distance. For the Pacific area, higher moisture increase is located over the Gulf of Alaska, being lower over the rest of the source. It is important to highlight that the value of the growth for the moisture uptake over the sources shows more than the double during the occurrence of ARs systems, comparing with climatological values.
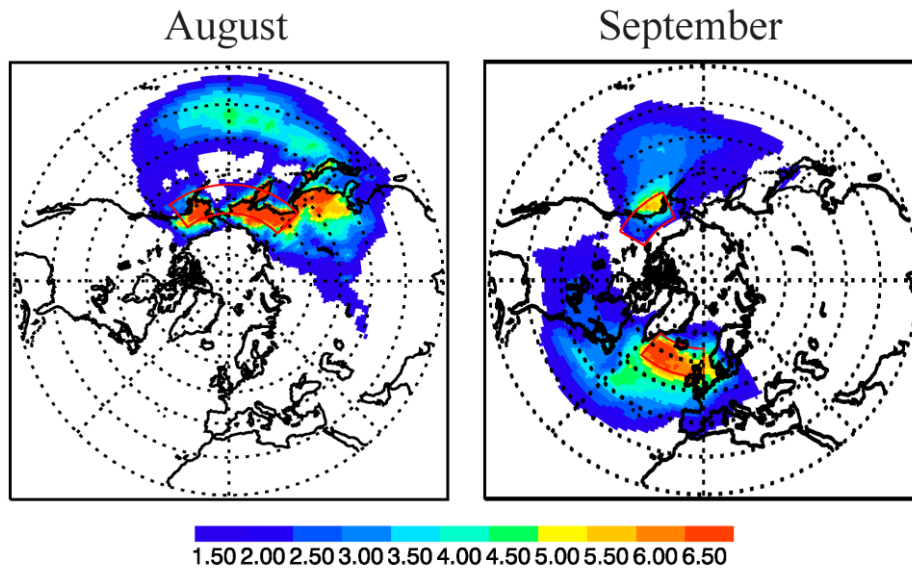

Figure 3. Anomaly for the moisture sources ((E-P)$_{AN}$>0 regions) for August and September for the regions of maximum ARs occurrence (red boxes) calculated for those days of ARs occurrence and referred to the climatological value over the period 1997-2014. Scale in mm/day.

4. Conclusions

In this work the origin of moisture feeding up the ARs affecting the Arctic was analysed for August and September. Areas of maximum ARs occurrence for the Arctic region are mainly located over the North Pacific (for August and September, with different longitudinal extension) and the North Atlantic (in September).

Moisture sources for the areas of maximum ARs occurrence were analysed and the results point to that the main moisture sources in August are located over continental areas of East Eurasia and Alaska for the Pacific area of maximum occurrence, and for September for both areas (Atlantic and Pacific) the moisture sources are located mainly over the ocean, to the southwest of the region itself.

For those days of ARs occurrence, moisture sources appear highly intensified, showing values that exceed more than twice the climatological value in some regions. In general, higher intensifications occur over the regions object of the study and decrease with the distance.

Author Contributions: R.N. and L.G. conceived and designed the experiments; K.P. performed the experiments; R.N., M.V. and K.P. analysed the data; M.V. and R.N. wrote the paper..

Conflicts of Interest: The authors declare no conflict of interest. The founding sponsors had no role in the design of the study; in the collection, analyses, or interpretation of data; in the writing of the manuscript, and in the decision to publish the results.

Abbreviations

The following abbreviations are used in this manuscript:

AR: Atmospheric River
E: Evaporation
ECMWF: European Centre for Medium-Range Weather Forecasts
IVT: Vertically integrated horiontal water vapour transport
P: Precipitation

References

1. Cavalieri, D.J.; Parkinson, C.L. Arctic sea ice variability and trends, 1979–2010, *The Cryosphere* **2012**, *6*, 881-889, doi:10.5194/tc-6-881-2012.

2. Comiso, J.C.; Hall, D.K. Climate trends in the Arctic as observed from space. *WIREs Clim Change* **2014**, *5*, 389–409, doi:10.1002/wcc.277

3. Comiso, J.C.; Parkinson, C.L.; Gersten, R.; Stock, L. Accelerated decline in the Arctic sea ice cover. *Geophys. Res. Lett.* **2008**. *35*, L01703, doi:10.1029/2007GL031972.

4. Parkinson, C.L.; DiGirolamo, N.E. New visualizations highlight new information on the contrasting Arctic and Antarctic sea-ice trends since the late 1970s. *Remote Sensing of Environment* **2016**, *183*, 198-204, doi:10.1016/j.rse.2016.05.020

5. Stroeve, J.C.; Kattsov, V.; Barrett, A.; Serreze, M.; Pavlova, T.; Holland, M.; Meier,W.N. Trends in Arctic sea ice extent from CMIP5, CMIP3, and observations. *Geophys. Res. Lett.* **2012**, *39*, L16502, doi: 10.1029/2012GL052676.

6. Serreze, M.C.; Holland, M.M.; Stroeve, J. Perspectives on the Arctic's Shrinking Sea-Ice Cover. *Science* **2007**, *315*, 1533–1536, doi: 10.1126/science.1139426.

7. Mortin, J.; Svensson, G.; Graversen, R.G.; Kapsch, M.L.; Stroeve, J.C.; Boisvert, L.N. Melt onset over Arctic sea ice controlled by atmospheric moisture transport. *Geophys. Res. Lett.* **2016**, *43*, 6636–6642, doi: 10.1002/2016GL069330.

8. Zhang, X.; He, J.; Zhang, J.; Polyakov, I.; Gerdes, R.; Inoue, J.; Wu, P. Enhanced poleward moisture transport and amplified northern high-latitude wetting trend. *Nat. Clim. Chang.* **2012**, *3*, 47–51, doi: 10.1038/nclimate1631.

9. Simmond, I.; Keay, K. Extraordinay September Arctic sea ice reductions and their relationship with storm behavior over 1979-2008. *Geophys. Res. Lett,* **2009**, *36*, L19715, doi:10.1029/2009GL039810.

10. Zhu, Y.; Newell, R.E. A proposed algorithm for moisture fluxes from atmospheric rivers. *Mon. Weather Rev.,* **1998** *126*, 725–735, doi:10.1175/1520-0493(1998)126<0725:APAFMF>2.0.CO;2.

11. Gimeno, L.; Dominguez, F.; Nieto, R.; Trigo, R.; Drumond, A.; Reason, C.J.C.; Taschetto, A.S.; Ramos, A.M.; Kumar, R.; Marengo, J. Major mechanisms of atmospheric moisture transport and their role in extreme precipitation events. *Annu. Rev. Environ. Resour.* **2016**, *41*, 3.1-3.25, doi:10.1146/annurev-environ-110615-085558.

12. Ralph, F.M.; Neiman, P.J.; Wick, G.A.; Gutman, S.I.; Dettinger, M.D.; Cayan, D.R.; White, A.B. Flooding in California's Russian River: Role of atmospheric river. *Geophys. Res. Lett.* **2006**, *33*, L13801, doi:10.1029/2006GL026689.

13. Neiman, P.J.; Ralph, F.M.; Wick, G.A.; Lundquist, J.D.; Dettinger, M.D. Meteorological characteristics and overland precipitation impacts of atmospheric rivers affecting the West Coast of North America based on eight years of SSM/I satellite observations. *J. Hydrometeor.* **2008**, *9*, 22–47, doi:10.1175/2007JHM855.1

14. Leung, L.R.; Qian Y. Atmospheric rivers induced heavy precipitation and flooding in the western U.S. simulated by the WRF regional climate model. *Geophys. Res. Lett.* **2009**, *36*, L03820, doi:10.1029/2008GL036445.

15. Gimeno, L.; Nieto, R., Vázquez, M.; Laver, D.A. Atmospheir river:a mini-review. *Front. Eart Sci.* **2014**, *2*, 2.1-2.6, doi:10.3389/feart.2014.00002

16. Sorteberg, A.; Walsh, J. E. Seasonal cyclone variability at 70°N and its impact on moisture transport into the Arctic, *Tellus A* **2008**, *60*, 570–586, doi: 10.1111/j.1600-0870.2008.00314.x

17. Baggett, C.; Lee, S.; Feldstein, S. An Investigation of the Presence of Atmospheric Rivers over the North Pacific during Planetary-Scale Wave Life Cycles and Their Role in Arctic Warming. *J. Atmos. Sci.* **2016**, *73*, 4329–4347, https://doi.org/10.1175/JAS-D-16-0033.1

18. Guan, B.; Waliser, D.E. Detection of atmospheric rivers: Evaluation and application of an algorithm for global studies. *J. Geophys. Res. Atmos.* **2015**, *120*, 12,514–12,535, doi:10.1002/ 2015JD024257.

19. Dee, D.P.; Uppala, S.M.; Simmons, A.J.; Berrisford, P.; Poli, P.; Kobayashi, S.; Andrae, U.; Balmaseda, M.A.; Balsamo, G.; Bauer, P.; et al. The ERA-Interim reanalysis: Configuration and performance of the data assimilation system. *Q. J. R. Meteorol. Soc.* **2011**, *137*, 553–597.

20. Stohl, A.; James, P.A. A Lagrangian Analysis of the Atmospheric Branch of the GlobalWater Cycle. Part I: Method Description, Validation, and Demonstration for the August 2002 Flooding in Central Europe. *J. Hydrometeorol.* **2004**, *5*, 656–678.

21. Stohl, A.; James, P.A. A Lagrangian Analysis of the Atmospheric Branch of the GlobalWater Cycle. Part II: Moisture Transports between Earth's Ocean Basins and River Catchments. *J. Hydrometeorol.* **2005**, *6*, 961–984.

22. Numagati, A. Origin and recycling processes of precipitation water over the Eurasian continent: Experiments using an atmospheric general circulation model. *J. Geophys. Res.* **1999**, *104*, 1957–1972, doi: 10.1029/1998JD200026.

23. Ramos, A.M.; Nieto, R.; Tomé, R.; Gimeno, L.; Trigo, R.M.; Liberato, M.L.R.; Lavers, D.A. Atmospheric rivers moisture sources from a Lagrangian perspective. *Earth Syst. Dynam.* **2016**, *7*, 371-384, https://doi.org/10.5194/esd-7-371-2016.